

Multi-object high-resolution echellette spectroscopy with IMACS

Brian M. Sutin and Andrew McWilliam

Carnegie Observatories, 813 Santa Barbara St., Pasadena, CA 91101.

ABSTRACT

By adding a prism-cross-dispersed echellette grating as an optional module to the Inamori Magellan Areal Camera and Spectrograph (IMACS), complete spectra from 3400 to 11000Å of 15 simultaneous objects may be achieved with a resolution of $R = 21,000$ for a projected 0.5-arcsec slit width and a 5.0-arcsec slit length. The additional cost of this module is on the order of \$50,000.

This echellette module (IMACS-E) is intended for studies of stellar abundances where the targets are sufficiently dense over the 15 arcmin IMACS field of view to take advantage of the multi-slit capability. Such applications include the study of Galactic bulge stars, stars in local group galaxies, stars in Galactic globular and open clusters, and the integrated light of extra-galactic globular cluster systems.

Keywords: spectroscopy, multi-object, high-resolution, echellette, abundances,galactic bulge,local group galaxies,globular clusters

1. INTRODUCTION

IMACS^{1,2} is an optical spectrograph with a grating-driven camera and a grism-driven camera. The grating-driven camera has a 15×15-arcmin field of view on the sky, imaged onto an 8192-pixel × 8192-pixel CCD detector array, resulting in a scale of 9 pixels per arcsec.

By adding a cross-dispersing prism in front of the grating, orders may be separated on the detector far enough to allow a slit length sufficient for reliable sky subtraction. Because of the cross-dispersion, the spectra will not be contaminated with light from adjacent orders, which is particularly important for stellar abundance work. In Figure 1 we show the IMACS optical layout and the location of the proposed echellette module. Figure 2 shows a detailed view of the echellette module.

The echellette addition to IMACS allows the unique combination of two usually disparate spectrograph characteristics: high resolution without cross-order contamination, and a multi-slit, wide-angle field of view. Perfect astronomical objects for study are any stars or stellar groups with sufficient density on the sky. Examples of such objects are Galactic bulge stars, stars in local group galaxies, stars in Galactic globular and open clusters, and extra-galactic globular clusters.

In the instrument addition to IMACS proposed here, the slit length has been chosen to be 5.0 arcsec, which should be more than adequate for the typical 0.5 to 0.8-arcsec seeing conditions expected for the Magellan telescopes. A 245 lines/mm, 37-degree blaze-angle grating ruling, available from Thermo RGL (Richardson Grating Lab), produces the spectrum from 3400 to 11000Å in 10 orders at a resolution of $R=50,000/\text{pixel}$, or $R=21,000/\text{projected } 0.5\text{-arcsec slit}$. Thus, in its standard operating mode the IMACS echellette, IMACS-E, will obtain simultaneous spectra of up to 15 objects, each from 3400 to 11000 Å.

The ruled area of the grating is 160 mm wide by 214 mm long, so while the grating is wide enough for the 150 mm beam, the grating is short of the 294 mm required to fit the entire beam. The light loss from vignetting of the grating is 20 percent.

Further author information: (Send correspondence to B.S.)

B.S.: E-mail: sutin@ociw.edu

A.M.: E-mail: andy@ociw.edu

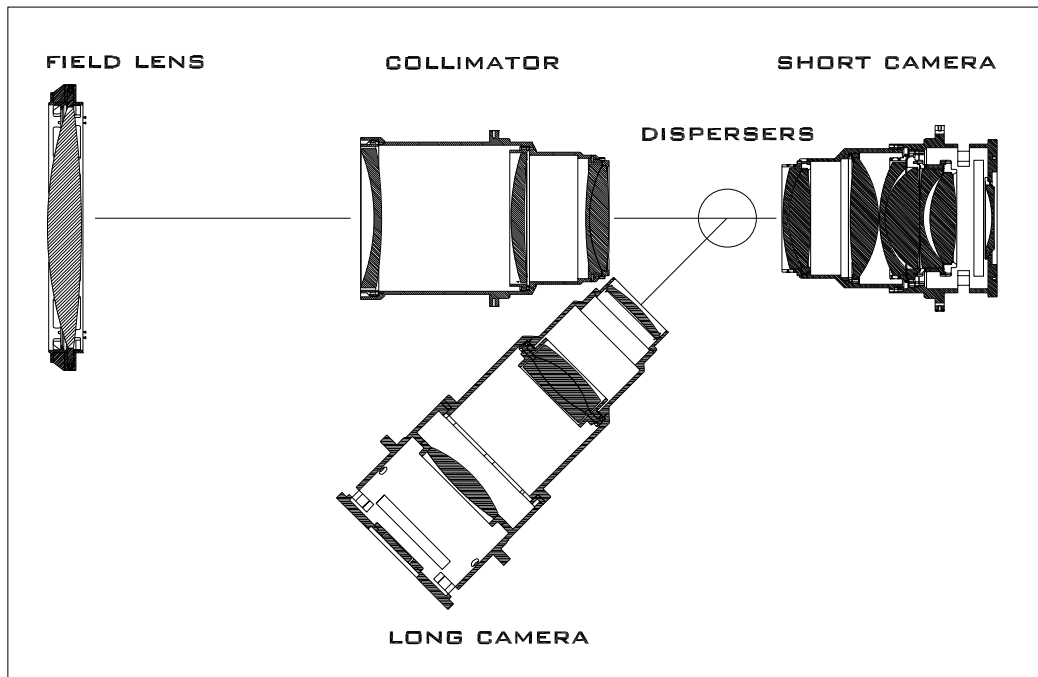


Figure 1 The IMACS optics. Shown are the field lens and collimator at the left, the short camera to the right, and the long camera at a 45-degree spectrograph angle below. The echellette module is located at the drawn circle.

The per-slit dispersion appears high because the large tilt of the grating provides anamorphic demagnification, which makes the slit appear narrower at the camera. Near the center of the field the anamorphic demagnification in the dispersion direction is 1.91; this projection factor also provides a significant boost to the areal coverage of the IMACS-E mode.

By giving up some portions of the spectra at the infrared end of the echellette patterns, the spectra can be shifted on the sky in the dispersion direction to give a large area of sky for placing object-slits; a region $\sim 10 \times 15$ -arcmin provides complete coverage up to $\sim 5000\text{\AA}$, with increasing loss at redder wavelengths.

The instrument will be made considerably more versatile with the use of order-separating filters. The addition of 6.5×6.5 inch filters in the converging beam of the long camera will permit an observer to restrict the spectra to wavelength regions of particular interest; this will make space available in the cross-dispersion direction, so that more objects may be observed in one exposure.

It should be noted that order separating filters provide half an order to the red and half an order blueward of the target spectral region, due to the nature of the echellette format. This effect limits the space savings in the cross-dispersion direction.

The wavelength restriction may be chosen to select several orders per object, such as in the case where only the blue or red regions are of interest. For example 27 objects could be observed simultaneously in the region from ~ 3650 to 6000\AA , and 39 objects for ~ 5000 to 7600\AA .

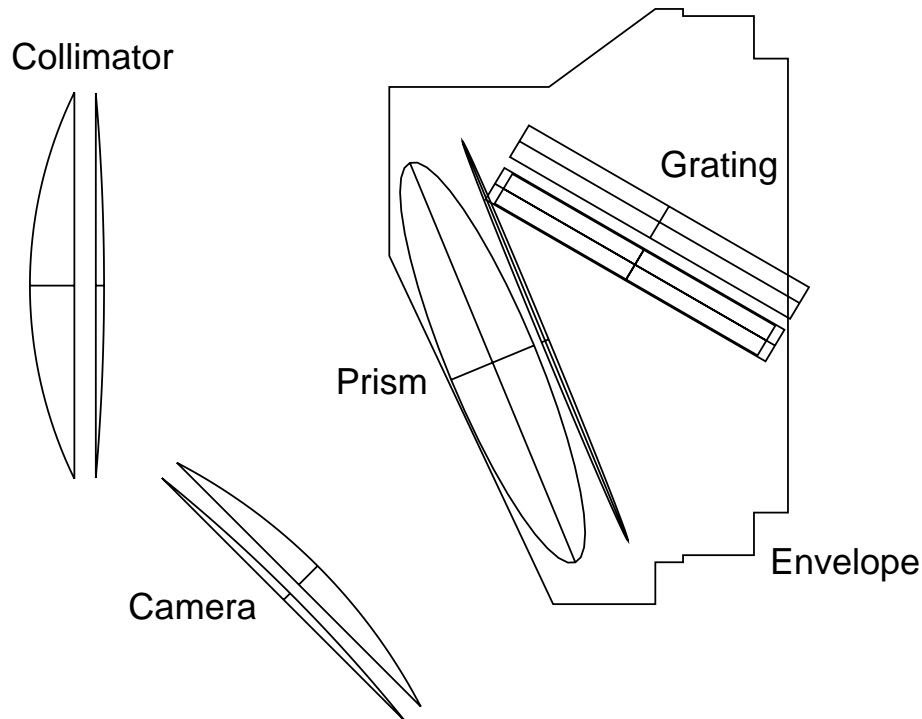


Figure 2 The Fused Silica design. The outlines are the front and back optical surfaces of the various optical elements. Only the last lens element of the collimator and the first lens element of the camera are shown. The front and back surfaces of the grating substrate are shown, along with an outline of the ruled region. Also shown is an outline of the available space. The grating substrate will have to be modified to fit within the space constraints.

The maximum packing would require a filter which separates out one single order. In this mode, with the 5-arcsec slits, ~ 11 arcsec apart to allow space for the two adjacent half-order pieces plus padding, approximately 80 objects could be observed simultaneously.

2. DESIGN

The most challenging part of the design is the packaging, since the echellette unit must fit into an already-designed IMACS multi-position wheel intended to carry simple mirrors, gratings, and grisms. Two designs now exist, with the only major difference being the makeup of the cross-dispersing prisms. After a computer search for optimal prism materials which would transmit down to at least 3650\AA , the two clear choices were either a single material of Fused Silica, or a prism doublet made up of two Ohara glasses, S-FSL5Y and PBM2Y. The echellette patterns for these two choices are shown in Figure 3 and Figure 4. The model using Fused Silica, with a prism angle of 13 degrees, will physically fit into the available space in the IMACS disperser-server wheel. On the other hand, the orders are not evenly spaced, resulting in a considerable waste of silicon real-estate at the blue end of the spectrum. The doublet prism, with 21.8 degrees of S-FSL5Y and 4.2 degrees of PBM2Y, has a much better order spacing, but only fits into the available space if one corner of the grating is removed. The resultant light lost is only about 4 to 5%; however, this would be offset by the 25% increase in the number of objects which could be observed in a single exposure. At the time of writing, the various angles in the double-prism model have not yet been optimized. The angles used here were found by a few hours of trial and error. We intend to computer optimize this design shortly.

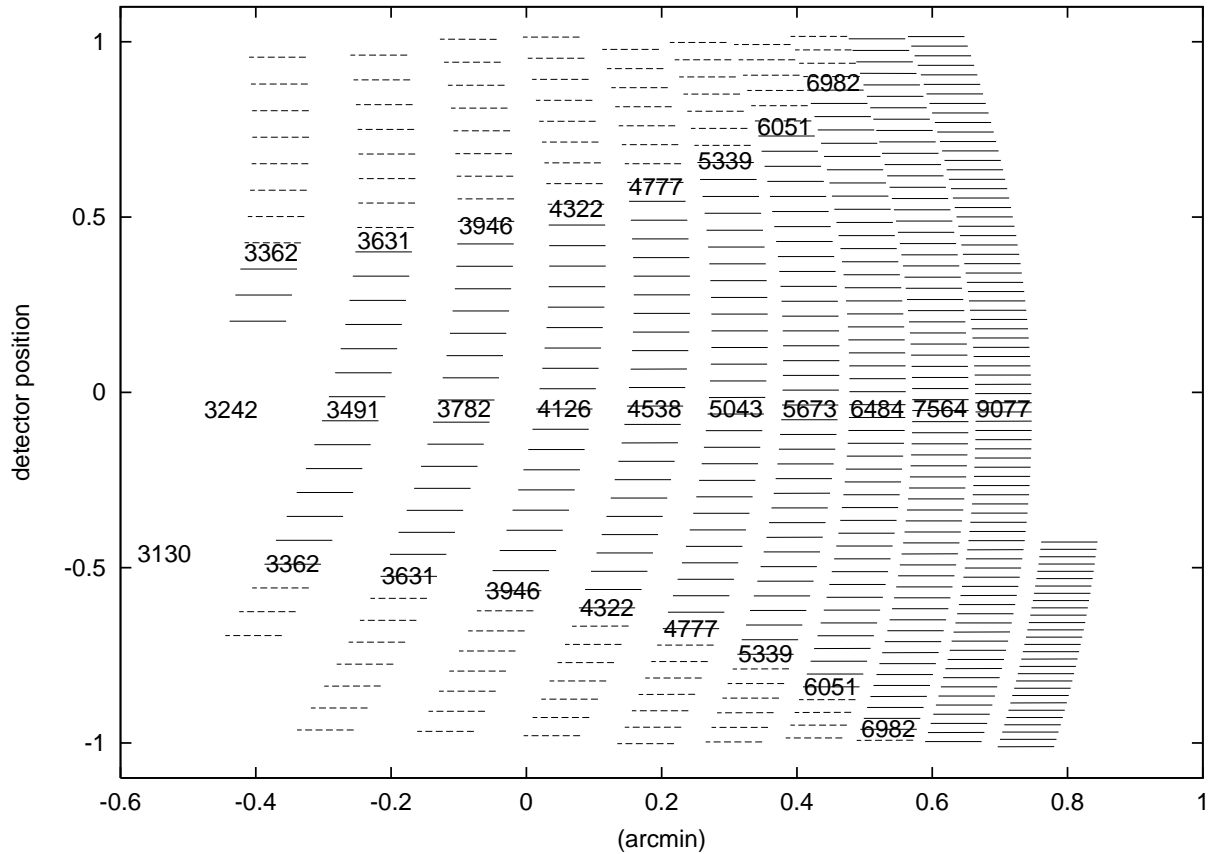


Figure 3 The predicted distribution of orders for a single object using the Fused Silica prism cross-disperser; central and half-power wavelengths, in Ångstroms, are indicated for each order. Note that the unit of measure for the ordinate scale is the half length of the detector.

3. CHEMICAL EVOLUTION WITH THE IMACS CROSS-DISPERSED ECHELLETTE

Detailed chemical abundance patterns can provide an extremely useful tool for understanding the formation history of star systems. Other than H, He, Li, Be and B, elements are principally synthesized by stars; however, different stars produce elements with various timescales and with characteristic abundance patterns, which ultimately depend on the details of the nuclear reaction networks in operation. By measuring the detailed composition of present-day stars in a system, we may infer the evolutionary timescale and the kinds of stars which produced the elements. The elemental abundance patterns form a kind of fossil record of past star formation.

For example, the abundance pattern of neutron-capture elements like Sr, Y, La, Ba, and Eu can be produced by core-collapse supernova (SN) explosions of massive stars (type II), with progenitor lifetimes of a few million years. Alternatively, low-mass stars can produce these elements on timescales of a few billion years, but in different proportions. The alpha elements O, Mg, Si, S, Ca, and Ti are thought to be made mostly by type II SN, whereas type Ia SN (arising from long-lived progenitors) produce relatively little of these elements. The abundances of some odd-numbered elements, like Mn and Cu, appear to be sensitive to the metallicity of the progenitor SN. For synthesis of neutron-capture elements in low-mass stars, the Ba/Y ratio is sensitive to the progenitor metal-content.

IMACS-E with its 10×15 arc minute field, is an excellent instrument for learning about the chemical evolution and formation history of nearby stellar systems. The capability to acquire high-resolution spectra over such a

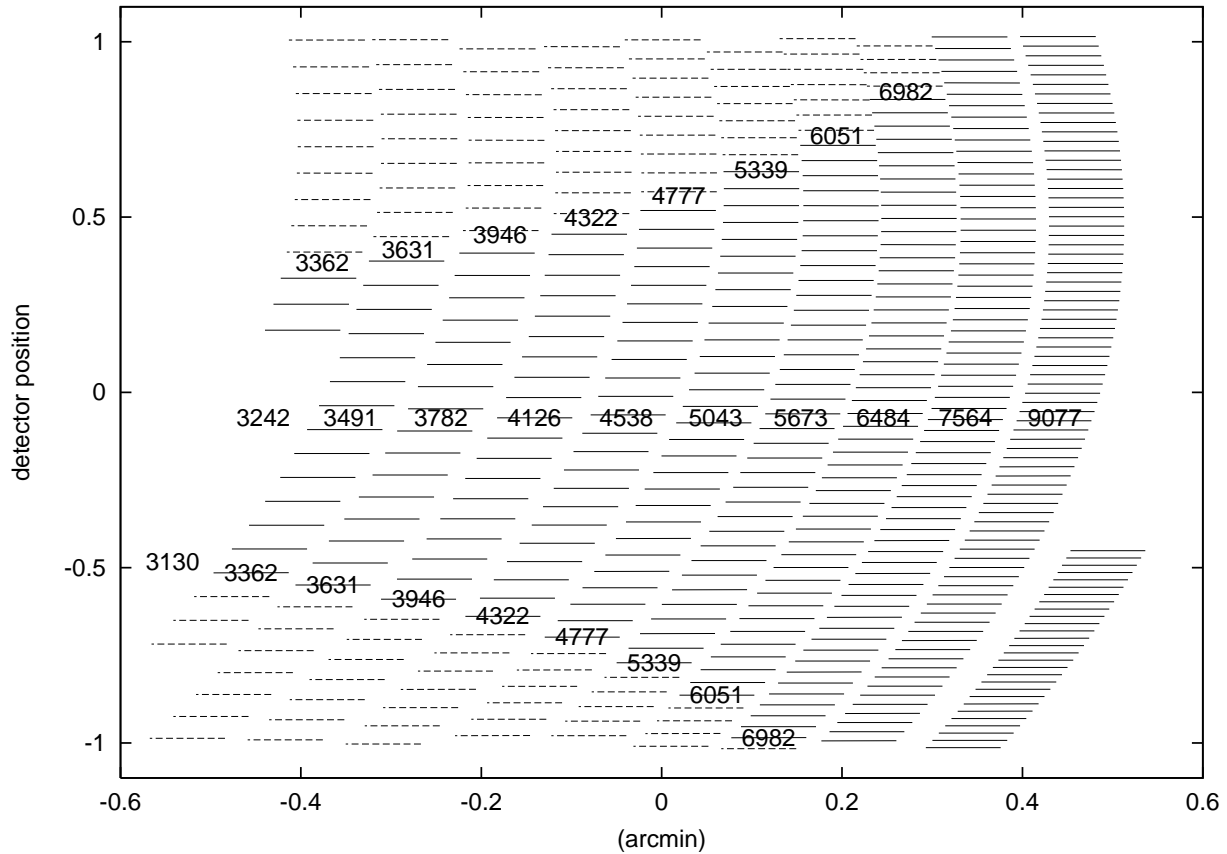


Figure 4 The predicted distribution of orders for a single object using the prism doublet cross-disperser, utilizing O'Hara S-FSL5Y and PBM2Y glasses. The central and half-power wavelengths, in Ångstroms, are indicated for each order. Note that the unit of measure for the ordinate scale is the half length of the detector.

large field of 15 to 30 objects simultaneously will have a substantial impact on our understanding of the nearby universe. These local systems, where individual stars can be analyzed in detail, will be key to unraveling the formation and evolution of distant galaxies where individual stars cannot be resolved.

Much of our current understanding of chemical evolution is based on the elemental composition of stars in our Galaxy, not too far from the sun. Clearly, it would be a good idea to extend the realm of understanding to include nearby star systems or galaxies, where the environment may be very different than the solar neighborhood. Such places include the bulge of our Galaxy, the Large and Small Magellanic Clouds, as well as other galaxies within the Local Group. Red giant stars in these systems are especially useful probes because they are bright, their progenitors can live for as long as the Universe, and their low temperatures permit absorption lines from many elemental species to be measured.

3.1. Detailed Composition of Stars in Local Group Spheroidal Galaxies

Dwarf spheroidal galaxies (dSphs) are apparently simple systems, potentially the building-blocks of giant galaxies. Their low mean metallicity suggests that relatively little chemical enrichment has occurred over the life of these systems; however, unlike globular clusters, most local group dSphs show evidence of a metallicity dispersion³.

The low metallicities of dSphs are interpreted as due to gas loss from these low-density, low-mass, systems, which brought star formation and chemical enrichment to a muted end. Thus, these systems can offer a glimpse

at chemical enrichment much less advanced than has occurred in the solar neighborhood, and can provide an interesting test of the chemical evolution paradigm.

Abundances for a handful of red giant stars in dSphs have been obtained^{4,5}, but only the brightest stars in a few galaxies have been studied so far. In order to obtain a more complete understanding it will be necessary to study many tens or a hundred stars per galaxy; this is particularly relevant because of the dSphs metallicity dispersion. Detailed chemical compositions have not yet been attempted for important dSphs accessible from the southern hemisphere (e.g. Carina and Fornax).

Carina is particularly interesting dSph, as it exhibits clear evidence of multiple epochs of star formation^{6,3}, with multiple turn-offs and a red clump and horizontal branch; these features indicate the presence of populations with vastly different ages, in the range 3 to 15 Gyr (see Figure 5).

The distinct sub-populations make it possible to measure the nucleosynthetic output from a star formation burst of a known age, assuming that the younger populations are composed of material synthesized by stars in the older groups. Elemental abundances observed in these sub-populations can be used to directly confront theoretical nucleosynthesis yields.

Measurement of the chemical composition of the dSph stars is aimed at addressing a number of questions, some of which follow: What does the chemical composition of the different dSphs look like, and are they all similar? Are the composition trends tight, or is there dispersion, which might indicate inhomogeneous evolution or incomplete mixing? How do the trends compare to the solar neighborhood, or other places in the Galaxy? Do the compositions of stars in the dSphs conflict with our present understanding of chemical evolution, or provide constraints on the nucleosynthetic sites of particular elements? To what extent can we constrain the theoretical nucleosynthesis yields using dSphs?

What is the range of [Fe/H] present in dSphs, and what are the age-metallicity relations? Are there any extreme metal-poor stars in dSphs ($[\text{Fe}/\text{H}] \leq -3.0$), or is there a lower limit to [Fe/H]? What constraint does this have on the formation history of dSphs, or chemical enrichment prior to population II? What is the source of the high frequency of carbon stars among dSphs? How do we understand this in the context of the hierarchical accretion scenario for building giant galaxies, and the halo of our Galaxy?

Present high resolution abundance spectra for the brightest dSph stars require long exposures: 1 to 4 hours with Keck. Obviously the ability to acquire 15 spectra at once will provide an enormous advantage. Given that the metal-poor stars in the dSphs have few useful lines beyond a wavelength of approximately 6000Å, and because these stars have much reduced flux below 3800Å a blocking filter to isolate the 3800–6000Å band would permit the acquisition of most of the useful spectral region, but allow an increase in the maximum number of objects from 15 to 32 per exposure. The IMACS-E field, at $\sim 10 \times 15$ arcmin, is well matched to the angular size of local group dSphs, e.g. Carina $R_{\text{core}}=9$ arcmin, $R_{\text{tidal}}=29$ arcmin, Fornax $R_{\text{core}}=14$ arcmin, $R_{\text{tidal}}=71$ arcmin.

Furthermore, the resolving power, at $R \sim 21,000$, is ideal for the abundance analysis of metal-poor stars present in dSphs. In Figure 6 we show spectra ($R=22,000$ and $S/N=30$) of three metal-poor stars in the Galactic halo used to perform detailed abundance analysis. These spectra show lines from a variety of elemental species and are expected to resemble those of the dSph stars.

3.2. Chemical composition of stars in the Galactic bulge

The Galactic bulge is the only metal-rich spheroidal system presently accessible to high resolution spectroscopy and abundance analysis, and thus offers a unique opportunity to study the fossil record of chemical enrichment in such systems. If giant elliptical galaxies and external bulges are to be understood from low spectral resolution integrated-light spectra it will be necessary to dissect at least one system on a star-by star basis at high spectral resolution; the Galactic bulge is presently the only candidate.

The general expectation is that bulges evolve rapidly to high metallicity, with an associated enhancement of alpha element abundances⁸. This picture is supported by studies of the integrated light spectra of giant elliptical galaxies, which show enhanced Mg features relative to the iron-peak⁹. If the bulge is oxygen enhanced and homogeneous then formation in a dissipative star burst is suggested. A multiple merger scenario would fit

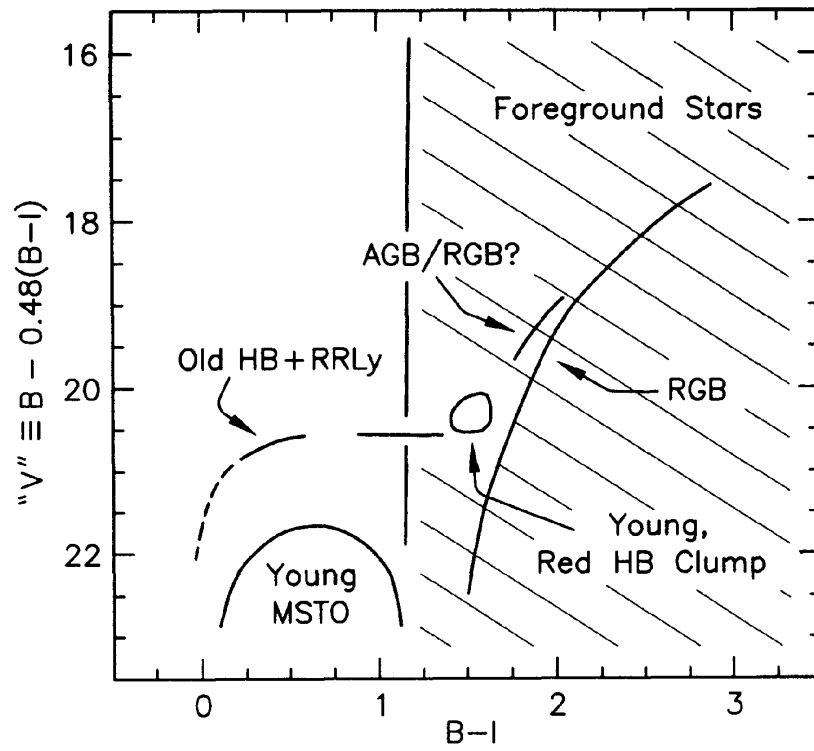
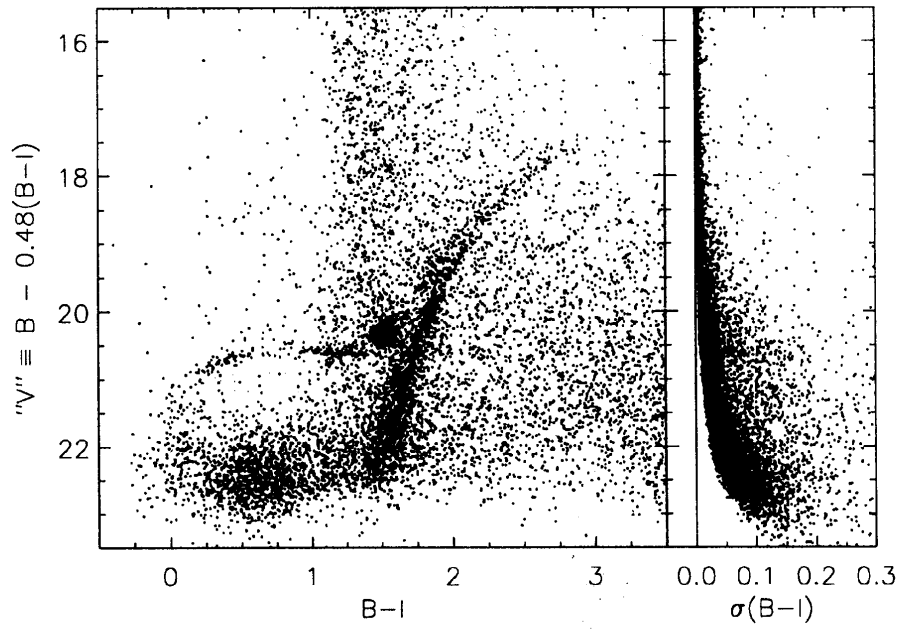


Figure 5: a: The *cmd* for the Carina dwarf spheroidal galaxy (Smecker-Hane et al 1994). b: Schematic diagram showing different age sub-populations in Carina.

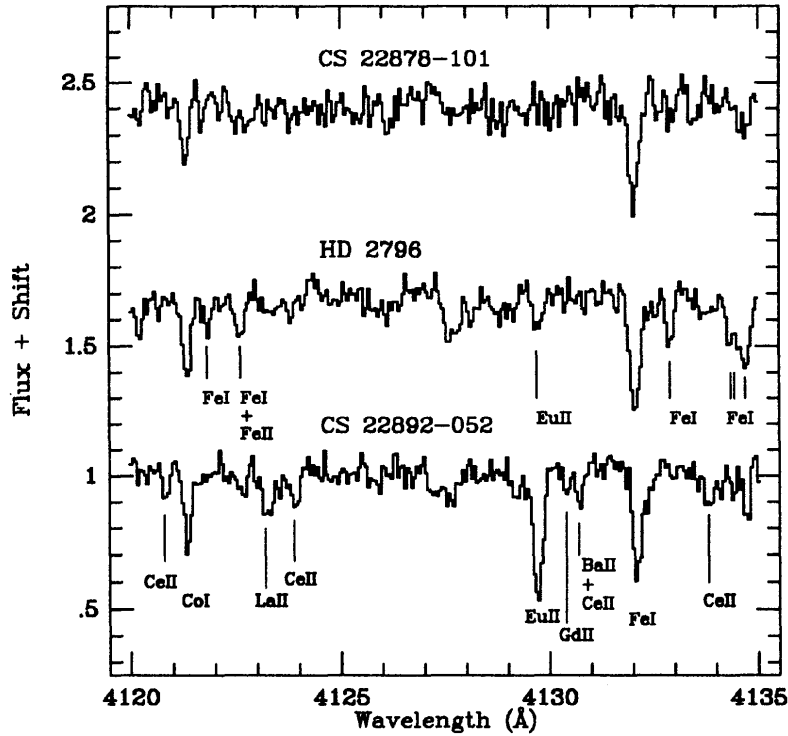


Figure 6 Spectra of three very metal-poor stars in the Galactic halo, with $R=22,000$, and $S/N \sim 30$ per pixel (from McWilliam et al 1995).

the facts better if observations indicate that the bulge contains many abundance subgroups, or large composition dispersions with metallicity. However, it would be difficult for such observations to identify formation by early, major-mergers.

With its ability to acquire spectra of many objects simultaneously IMACS-E will be a useful tool for high-resolution studies of the chemistry of the Galactic bulge; it will be most useful for acquiring spectra of large numbers of bulge red giant stars.

To date two high-resolution abundance studies of bulge stars have been performed^{10,11} for only a dozen stars. In Figure 7 we show a spectrum of a $[Fe/H] \sim -1$ bulge red giant star at $R=17,000$ and $S/N \sim 50$, near the H_α line; it is clear that somewhat more metal-rich stars would have plentiful continuum and be relatively free of line blanketing in this region. The low spectral resolution survey of Sadler et al (1996)¹² included over 400 stars, but only provided estimates for the overall metal content, made more uncertain due to the large reddening corrections.

IMACS-E could be used to measure the metal content of hundreds of Galactic bulge stars at high resolution, with reliable $[Fe/H]$ values, for red giant stars up to $[Fe/H] \sim 0.0$ dex. The high resolution spectra would enable reddening-independent temperatures to be determined for each star, from the excitation of Fe I lines.

The $[Fe/H]$ values will test the claim by Rich (1990)¹³ that the bulge metallicity function follows the Simple, closed-box, model of chemical evolution, and does not suffer from the paucity of metal-poor stars (the G-dwarf problem) present in the solar neighborhood. The *yield* derived from the Simple model fit to the $[Fe/H]$ function will be a useful input parameter for chemical evolution models of other systems.

Measurement of the $[Fe/H]$ function in the Galactic bulge at several locations will determine whether there is a radial metallicity gradient. Gradients have been claimed in the past for the outer regions, from -3° to

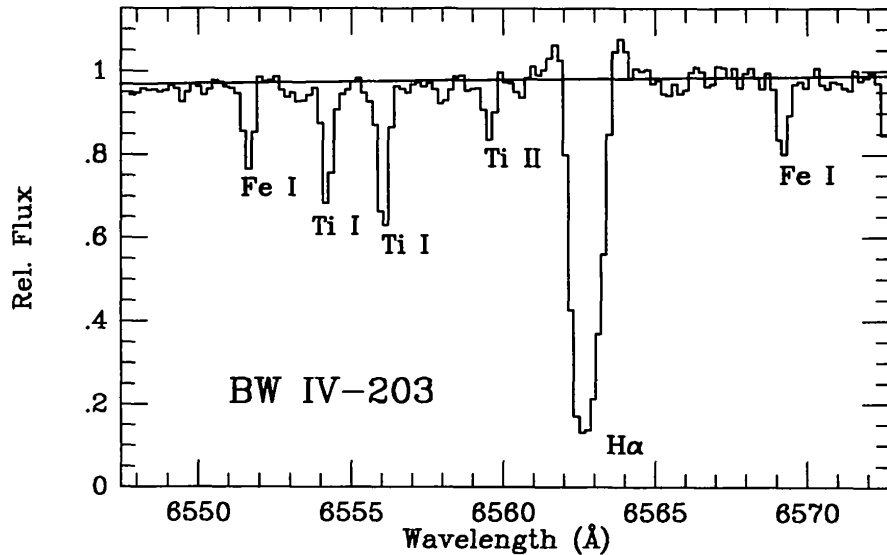


Figure 7 Spectra of a metal-poor, $[\text{Fe}/\text{H}]=-1$, Galactic bulge K giant $R=17,000$, and $S/N\sim 50$ per pixel (from McWilliam & Rich 1994). The solid line shows the local continuum. The Ti II line at 6559\AA has an equivalent width of $55\text{m}\text{\AA}$.

-12° latitude, based on the slope of the red giant branch photometric colors^{14,15}; however Ramirez et al (2000)¹⁶ found no evidence of a gradient from -0.2° to -4° , based on infrared spectroscopy. It is possible that the putative metallicity gradients are caused by a change in composition with radius. For example the results of Terndrup¹⁴ are probably sensitive to the Ti/Fe ratio of his stars, due to the blanketing effect of the TiO molecule. Since Ti is a minor species its abundance does not change the overall metallicity by a measurable amount, but it can greatly affect photometric colors due to TiO blanketing.

With the large number of available lines from atomic Ti it will be possible to measure Ti/Fe with spectra from IMACS-E; however, lines of other species will be blended in metal-normal red giant stars at the IMACS-E resolution, and it will be necessary to use the Magellan Echelle spectrograph (MIKE) for such detailed abundance studies in these stars. At lower metallicities, say $[\text{Fe}/\text{H}]<-0.5$ dex, IMACS-E spectra will be sufficient for measuring abundances of most species, thanks to the reduced line blanketing and increased continuum.

With regard to the chemical composition in the low-metal tail $-2<[\text{Fe}/\text{H}]<-1$ IMACS-E would be able to measure the trends of various abundance ratios with $[\text{Fe}/\text{H}]$; the density of red giant stars in this range is high enough that several objects will be available in a single exposure.

It will be interesting to know how the composition trends in the metal-poor bulge compare with the trends in the Galactic halo and disk populations, and whether differences can be attributed to the timescale of star formation and chemical enrichment. As indicated in the introductory paragraphs, various diagnostic element abundances (e.g. O, Ca, Mg, Si, Ca, Ti, Sr, Y, Ba, La, Eu) will constrain the mix of stars and hence the chemical evolution timescale for the bulge. The bulge composition information will also provide a test of the chemical evolution paradigm in an environment much different than other locations in the Galaxy.

Bulge red giant stars have much reduced flux at blue wavelengths, due to the relatively low temperatures and the high Galactic reddening. For this reason, IMACS-E will be most efficiently utilized for the bulge with a blocking filter to select only light from the orders in the interval $\sim 5000\text{--}7600\text{\AA}$; as mentioned previously, in this mode it will be possible to acquire spectra of up to 39 stars simultaneously.

3.3. Other Projects

We have provided some detail on two projects for which IMACS-E will be of great use. Other projects include: the study of the chemical composition of red giant stars in the LMC bar, and other densely populated regions of the Magellanic clouds; the composition of large numbers of stars in populous globular clusters such as ω Cen and 47 Tuc; radial velocity monitoring of large numbers of stars in Local Group dSph systems, in order to identify binaries and measure the intrinsic velocity dispersions for mass measurements; velocity dispersions of extra-galactic globular cluster systems, and the abundance analysis of the integrated light of extra-galactic globular clusters.

ACKNOWLEDGMENTS

The authors would like to acknowledge Alan Dressler, principle investigator of IMACS, and Bruce Bigelow, IMACS Instrument scientist. We would also like to thank Bruce Bigelow for providing Figure 1.

REFERENCES

1. A. Dressler, B.M. Sutin, & B.C. Bigelow, “*Science with IMACS on Magellan*”, SPIE, **4834**, 2002.
2. A. Dressler, & B.C. Bigelow, “*IMACS, the multi-object spectrograph and imager for Magellan 6.5m telescope: a status report*”, SPIE, **4841**, 2002.
3. M. Mateo, “*Dwarf Galaxies of the Local Group*”, ARAA, **36**, p. 435, 1998.
4. M.D. Shetrone, P. Côté, & W.L.W. Sargent, “*Abundance Patterns in the Draco, Sextans, and Ursa Minor Dwarf Spheroidal Galaxies*”, ApJ **548**, p. 592, 2001.
5. T.A. Smecker-Hane & A. McWilliam, “*The Complex Chemical Abundances and Evolution of the Sagittarius Dwarf Spheroidal Galaxy*”, ApJ, *submitted*, 2002.
6. T.A. Smecker-Hane, P.B. Stetson, J.E. Hesser, & M.D. Lehnert, “*The stellar populations of the Carina dwarf spheroidal Galaxy. 1: A New color-magnitude diagram for the giant and horizontal branches*”, AJ, **108**, p. 507, 1994.
7. A. McWilliam, G.W. Preston, C. Sneden, & L. Searle, “*Spectroscopic Analysis of 33 of the Most Metal Poor Stars. II*”, AJ, **109**, p. 2757, 1995.
8. F. Matteucci & E. Brocato, “*Metallicity distribution and abundance ratios in the stars of the Galactic bulge*”, ApJ, **365**, p. 539, 1990.
9. G. Worthey, S.M. Faber, & J.J. Gonzalez, “*Mg and Fe absorption features in elliptical galaxies*”, ApJ, **398**, p. 69, 1992.
10. A. McWilliam & R.M. Rich, “*The first detailed abundance analysis of Galactic bulge K giants in Baade’s window*”, ApJS, **91**, p. 74, 1994.
11. R.M. Rich & A. McWilliam, “*Abundances of stars in the galactic bulge obtained using the Keck Telescope*”, SPIE, **4005**, p. 150, 2000.
12. E.M. Sadler, R.M. Rich, & D.M. Terndrup, “*K Giants in Baade’s Window. II. The Abundance Distribution*”, AJ, **112**, p. 171, 1996.
13. R.M. Rich, “*Kinematics and abundances of K giants in the nuclear bulge of the Galaxy*”, ApJ, **362**, p. 604, 1990.
14. D.M. Terndrup, “*The structure and stellar population of the Galactic nuclear bulge*”, AJ, **96**, p. 884, 1988.
15. J.A. Frogel, G.P. Tiede, & L.E. Kuchinski, “*The Metallicity and Reddening of Stars in the Inner Galactic Bulge*”, AJ, **117**, p. 2296, 1999.
16. S.V. Ramirez, A.W. Stephens, J.A. Frogel, & D.L. Depoy, “*Metallicity of Red Giants in the Galactic Bulge from Near-Infrared Spectroscopy*”, AJ, **120**, p. 833, 2000.